IABSE CONGRESS

GHENT 2021

Structural Engineering for Future Societal Needs

International Associating for Bridge and Structural Engineering IABSE

Editors
H.H. (Bert) Snijder, Eindhoven University of Technology, Eindhoven, The Netherlands
Bart De Pauw, TUC RAIL, Brussels, Belgium and Ghent University, Ghent, Belgium
Sander van Alphen, Movares, Utrecht, The Netherlands
Pierre Mengeot, Besix, Brussels, Belgium

Publisher

IABSE

Jungholzstrasse 28

8050 Zurich

SWITZERLAND

Phone: +4143 443 97 65

Email: secretariat@iabse.org

www.iabse.org

ISBN: 978-3-85748-176-5

Please refer to this report as follows:

IABSE Congress Ghent 2021, Structural Engineering for Future Societal Needs, Congress Proceedings, Eds. H.H. Snijder, B. De Pauw, S. van Alphen & P. Mengeot, IABSE, Zurich, 2021

Proceedings

IABSE Congress Ghent 2021
Online event

IABSE Belgian Group
IABSE Dutch Group
GHENT UNIVERSITY

Analysis for Optimization of Spiral Reinforcement in Pre-Fabricated Bridge Columns

Lubos Rehounek, Jan Cervenka, Radomir Pukl

Cervenka Consulting s.r.o., Prague, Czech Republic

Contact: jan.cervenka@cervenka.cz

Abstract

Savings and optimization in the use of steel and concrete can significantly contribute to the reduction of CO2 emission and energy consumption, promoting a greener environment for the place we live. It has been shown that the use of multi-spiral reinforcement (MSR) in square or rectangular columns can significantly save the amount of steel for transverse reinforcement and yet can still achieve a higher structural performance than conventional tie reinforcement. The paper presents a validation of a numerical model for nonlinear analysis of novel multi-spiral reinforcement in prefabricated columns. The validated model will be used for the subsequent studies and optimization of the spiral reinforcement location, diameter and pitch. Selected arrangements of the multi-spiral reinforcements have been analysed to demonstrate their effectiveness in static and cyclic response.

Keywords: Spiral reinforcement; reinforced concrete columns; cycling loading; nonlinear simulation; finite element analysis.

1 Introduction

Savings and optimization in the use of steel and concrete can significantly contribute to the reduction of CO2 emission and energy consumption, promoting a greener environment for our planet. It has been shown by previous studies [1, 2] that the use of multi-spiral reinforcement (MSR) in square or rectangular columns can significantly save the amount of steel for transverse reinforcement and yet can still achieve a higher structural performance than conventional tie reinforcement. A higher structural performance means a further save in steel reinforcement and concrete can be made for a given structural performance. The multi-spiral column has an amount of transverse reinforcement only 80% the amount used in a conventional tied column but still shows a 29% higher axial strength than the conventional tied column. The multi-spiral column used only 69% the amount of transverse reinforcement used in the conventional tied column but still showed an 18% increase in lateral strength and a 59% increase in energy dissipation. These test results have demonstrated that concrete confined by multi-spiral reinforcement as a new form of confined concrete material can reduce the use of concrete and steel as compared with conventional confined concrete and hence promote savings in energy and CO_2 emission.

The paper presents nonlinear analysis of novel multi-spiral reinforcement for prefabricated columns. A special program module was developed for future simulations of spiral-reinforced concrete columns and optimization of reinforcement geometry.

2 Spiral reinforcement in prefabricated bridge columns

The main motivation behind introducing a spiral reinforcement is to reduce the overall reinforcement level while increasing structural resistance against transversal loads. The spiral reinforcement is also advantageous for the automation of the manufacturing process, which is especially appealing for prefabricated reinforced concrete elements. In practice, rectangular or square columns are, however, much more practical to and advantageous to use. Therefore, the design aims to use square columns with spiral reinforcement positioned into the rectilinear perimeter of the square so that the advantages of square columns can be combined with concrete confinement generated by the spiral reinforcement. The typical geometrical configuration of the spiral reinforcement is shown on Figure 1.

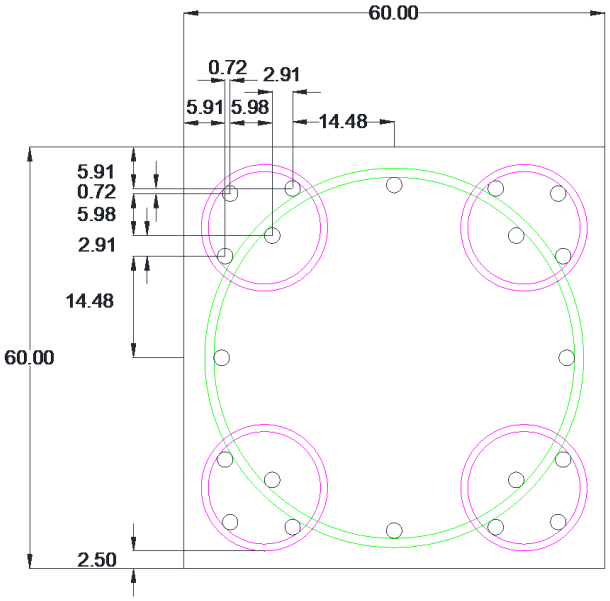

Figure 1. The geometrical configuration of spiral reinforcement inside of the analysed column [cm], all rebars are made of SD420W steel.

The used reinforcement bars displayed on Figure 1 were as follows:

- 4Ø9.5mm small spiral bars, outer diameter 180 mm, pitch 800 mm
- 1Ø16mm big spiral bar, outer diameter 540 mm, pitch 800 mm
- 20Ø22mm longitudinal bars

One of the advantages of the spiral reinforcement is also the confinement effect. Confinement represents a reduction in lateral displacement of concrete members by means of transverse reinforcement, therefore increasing the compressive strength of the concrete member. In the presented studies the fracture-plastic material model is used for this application and the model formulation including concrete confinement is presented in [3], [4] and [5].

Figure 2: The column with the spiral reinforcement tested in MATS (Multi-Axial Testing System) at NCREE laboratory in Taiwan.

3 Numerical model

The computational model was created in the ATENA Science software [4] that uses FEM to solve complex numerical problems. An image showing the geometry of the model is shown on Figure 3 and Figure 4. The used concrete material model is internally described as CC3DNonLinCementitious2 in the program, described in detail in Chapter 4.

The aim of the simulation was to develop a working program module for optimization of spiral reinforcement for future simulations. Calibrated simulations of large concrete members can potentially save a lot of material, laboratory space and time and therefore contribute towards decreasing the CO2 footprint.

The model simulates a shaking table real-scale test performed at NCREE, Taiwan. During the test,

displacement load is applied on the bottom moving block of the assembly to simulate an earthquake.

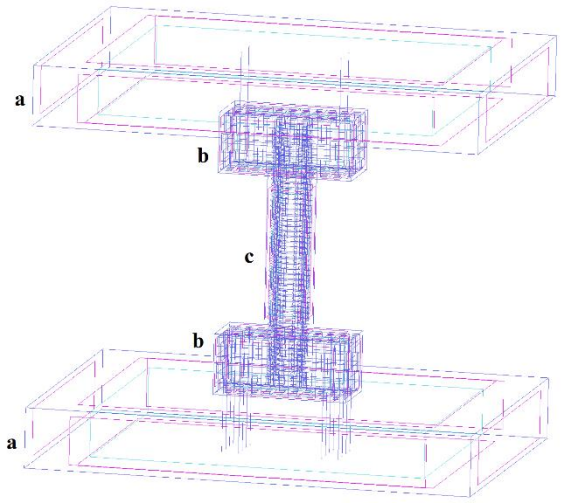

Figure 3. Geometrical model of the OY1 analysed column with multi-spiral reinforcement. a) stiff steel anchoring blocks (upper fixed, lower allowed to move in the direction of the load), b) reinforced concrete blocks, c) column with multi-spiral reinforcement. The column is 2400 mm tall, excluding the concrete anchoring blocks.

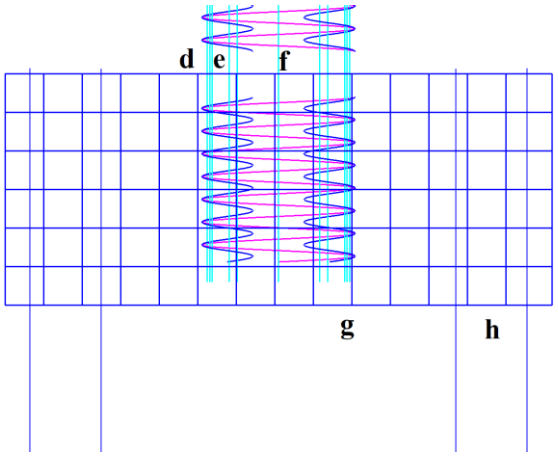

Figure 4. Detail of the foundation. d) longitudinal column reinforcement (20 bars), e) 4 small diameter spirals, f) central big-diameter spiral, g) reinforcement of the anchoring blocks and h) pre-stressing bars.

The loads were prescribed according to a true-scale experiment performed on a large multi-axial test machine (MATS, Taiwan). The displacement diagram that was used both in experiment and simulation and represents a cyclic earthquake load is shown on Figure 5.

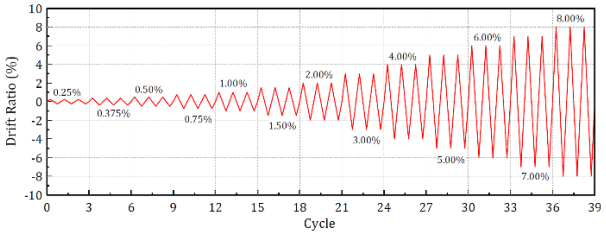

Figure 5: The prescribed cyclic displacement loading diagram. Drift ratio represents a ratio of column height to the lateral displacement.

The boundary conditions of the geometry are displayed on Figure 6. The model is constrained according to the laboratory conditions – z-axis movement of the column is allowed for pre-stressing (concrete compressive strength $f_c' = 48.26\ MPa$ and the pre-stressing pressure was $0.1 \times f_c'$) and x-axis movement is allowed for all bodies except for the upper steel anchor to simulate displacement loading. Other rotations and translations are not allowed. Note that only one peak of each cycle of the diagram (Figure 5) was modeled in the software to decrease the computational requirements (Figure 13).

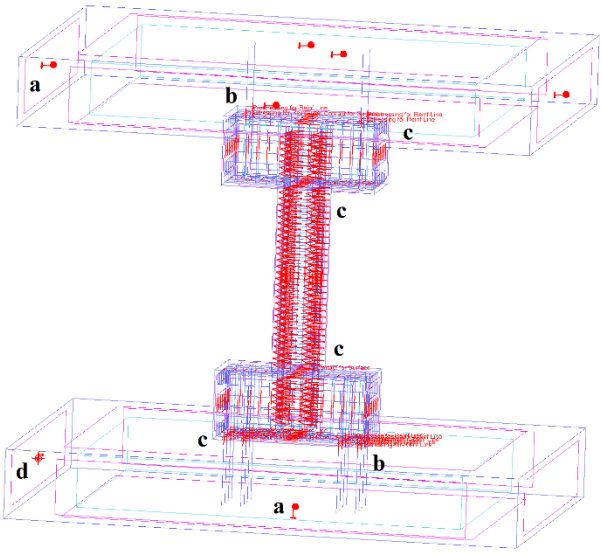

Figure 6. Boundary conditions of the model as shown in the FE preprocessor: a) fixed (upper) and moving (lower) steel stiff blocks, b) pre-stressing of the anchoring bars, c) fixed contacts between 3D elements, d) displacement load.

4 Material model for concrete and reinforcement

The nonlinear finite element analyses presented in this paper are performed with the software ATENA [4] using the combined fracture-plastic model for concrete of Červenka & Pappanikolaou (2008) [5].

The constitutive model formulation is based on the strain decomposition into elastic ε_{ij}^{e}, plastic ε_{ij}^{p} and fracture ε_{ij}^{f} components. The stress development is described by the rate equations reflecting the progressive damage (concrete cracking) and plastic yielding (concrete crushing):

$$\dot{\sigma}_{ij} = D_{ijkl} \cdot (\dot{\varepsilon}_{kl} - \dot{\varepsilon}_{kl}^{p} - \dot{\varepsilon}_{kl}^{f}) \tag{1}$$

The flow rule governs the evolution of plastic and fracturing strains:

$$\text{plastic model:} \quad \dot{\varepsilon}_{ij}^{p} = \dot{\lambda}^{p} \cdot m_{ij}^{p}, \qquad m_{ij}^{p} = \frac{\partial g^{p}}{\partial \sigma_{ij}}, \tag{2}$$

$$\text{practure model:} \quad \dot{\varepsilon}_{ij}^{f} = \dot{\lambda}^{f} \cdot m_{ij}^{f}, \qquad m_{ij}^{f} = \frac{\partial g^{f}}{\partial \sigma_{ij}}, \tag{3}$$

where $\dot{\lambda}^{p}$ is the plastic multiplier rate and g^{p} is the plastic potential function, $\dot{\lambda}^{f}$ is the inelastic fracturing multiplier and g^{f} is the potential defining the direction of inelastic fracturing strains. The multipliers are evaluated from the consistency conditions.

The model of Menetrey-Willam [6] is used for plasticity of concrete in multiaxial stress state in compression (Figure 7) with nonlinear hardening (Figure 8) and linear softening (Figure 9).

In tension, Rankine criterion for tensile fracture with exponential softening of Hordijk [7] – see Figure 10 – is used, where w_t stands for the crack width.

The stress softening in tension is determined using the crack band approach of Bažant & Oh [8] and analogically in compression according to Červenka et al. [9]. The crack band L_t as well as the crush band size L_c are adjusted with regard to the crack orientation approach proposed by Červenka & Margoldová [10]. This method is illustrated in Figure 11 and described by Eq. (4):

$$L_t' = \alpha \gamma L_t \quad \text{and} \quad L_c' = \gamma L_c \tag{4}$$

$$\gamma = 1 + (\gamma_{max} - 1)\frac{\theta}{45}, \quad \theta \in \langle 0; 45 \rangle,$$

$$\gamma_{max} = 1.5$$

The crack angle θ is taken as the average angle between crack direction and element sides.

The above formulation controls the strain localization accounting for the mesh size and the crack orientation. Parameter α is introduced to cover the localization effect due to the element type as reported recently in the work of Slobbe et al. [11]. In this study $\alpha = 1$ is used for low order elements with 2x2 integration scheme and $\alpha = 0.6$ for quadratic elements with 3x3 integration scheme.

Some additional features of cracked concrete included in the model, namely the reduction of compressive strength and shear stiffness degradation, often referred as a shear retention effect, should be mentioned due to their importance in problems dominated by shear failure.

The damage of concrete by cracks is reflected according to Bentz et al. [12] in the reduction factor r_c of the compressive strength f_c as follows:

$$\sigma_c = r_c \, f_c \tag{5}$$

$$r_c = \frac{1}{0.8 + 170\,\varepsilon_1}, \quad r_c^{lim} \le r_c \le 1.0$$

Where ε_1 is the tensile strain normal to the crack. The largest maximal fracturing strain is used for ε_1

and the compressive strength reduction is limited by $r_c^{\lim}$. In this work $r_c^{\lim}$ = 0.8 is considered.

The shear strength of the cracked surface is also considered according to the modified compression field theory (MCFT) by Bentz et al. [12]:

$$\sigma_{ij} \leq \frac{0.18\sqrt{f_c'}}{0.31+\frac{24\,w}{a_g+16}}; \quad i \neq j \tag{6}$$

Taking into account the crack width w and aggregate size a_g. Since MCFT does not offer shear stiffness, the authors proposed to relate the shear stiffness K_t^{cr}, oriented tangentially to the crack face, to the normal stiffness K_n^{cr} already defined by a crack opening law:

$$K_t^{cr} = s_F\, K_n^{cr} \tag{7}$$

The normal stiffness comes directly from the tensile softening law in Figure 10 as:

$$K_n^{cr} = f_t(w_t)/w_t \tag{8}$$

This makes the shear stiffness dependent on the crack opening displacement and independent of the mesh size. The scaling factor $s_F = 20$ was used in the presented analyses.

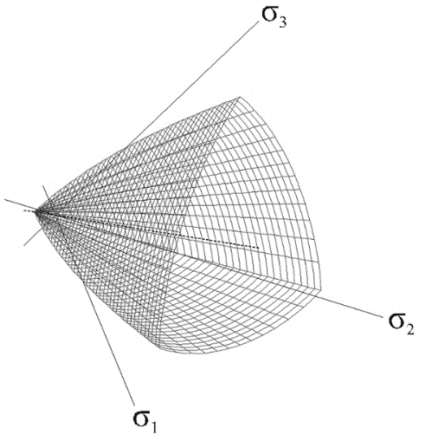

Figure 7. Visualization of the three-parameter Menetrey & Willam [6] three-parameter concrete failure criterion.

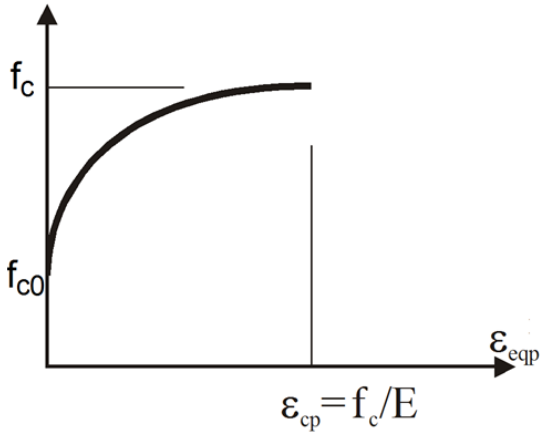

Figure 8. Hardening law for the plasticity model for concrete in compression.

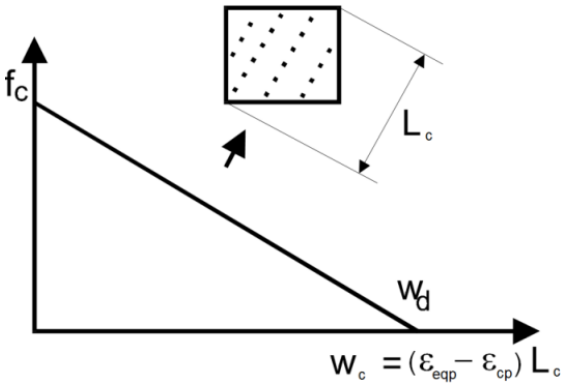

Figure 9. Softening law for the plasticity model for concrete in compression.

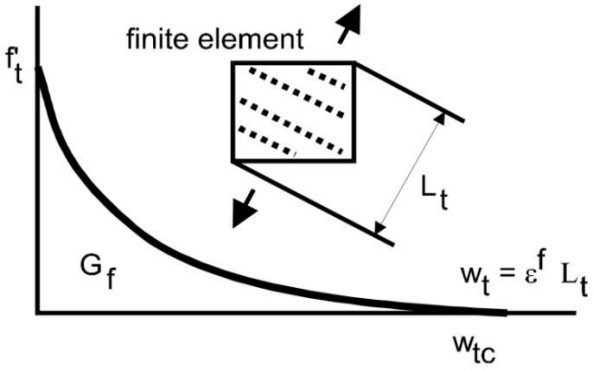

Figure 10: Crack opening law according to Hordijk [7].

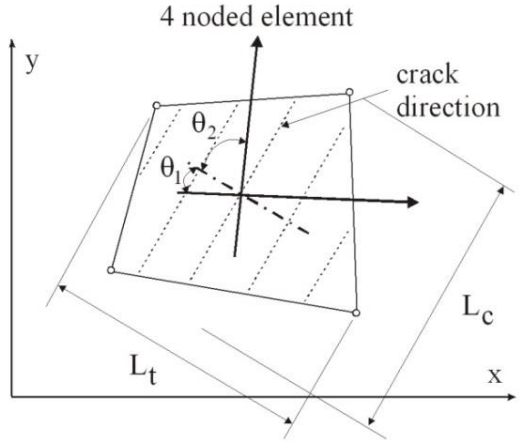

Figure 11. Crack band formulation.

The reinforcement is modelled using the embedded approach as for instance described in [13]. In this approach, a separate model is developed for the 3D concrete geometry and for the reinforcement. In the presented analyses, the reinforcement is modelled by truss elements that are embedded into the 3D solid elements. The compatibility in deformations is enforced through special constraint conditions as described in [13]. This approach enables the consideration of slip between reinforcement and concrete by introducing additional slip degrees of freedom to the finite element nodes belonging to the reinforcement as proposed by Jendele & Cervenka [14].

Cycling reinforcement bond model is used (see Figure 12) to simulate the reinforcement bond behavior during the cycling loading. The hysteretic response of the steel reinforcement material is modeled using Menegotto & Pinto model [15].

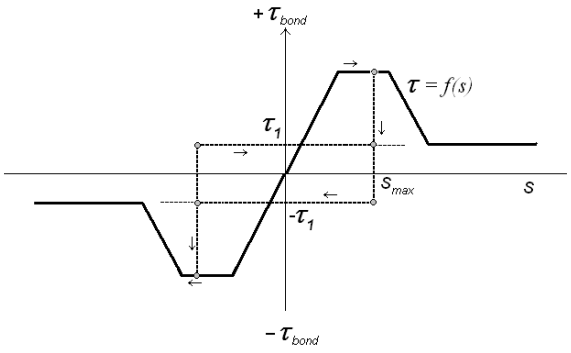

Figure 12: Reinforcement bond with cycling working diagram.

5 Modelling of cycling response

The cyclic response of the model is shown on Figure 13. The simulation follows the true displacement with acceptable accuracy. Failure of the model occurs at the same value of the displacement, although the peaks of reaction force do not exactly match measured force values.

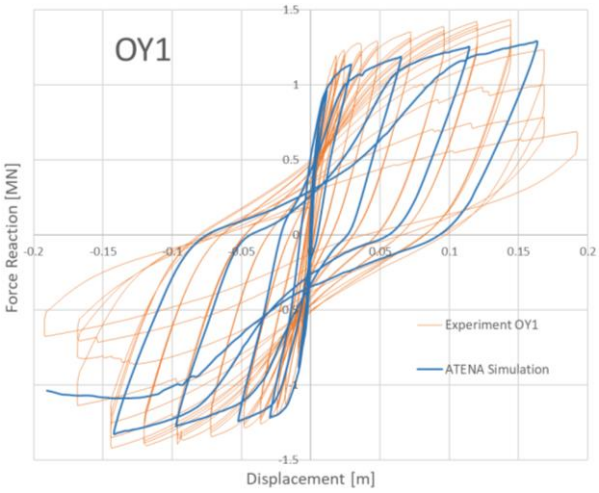

Figure 13: ATENA simulation of the OY1 cyclic loading experiment. Failure occurs within the same value of displacement, peaks of force subject to further minor refinement.

This could be a stiffness problem that requires either a model refinement and/or a geometry refinement as some parts of the model were simplified in order to reduce the computational requirements. Other possible explanation is that in order to achieve a match in the peaks of force, a different formulation of reinforcement behaviour, bond or confinement is necessary.

The failure of the model occurs by reinforcement fracture as shown on Figure 14. Corresponding reinforcement stresses are shown on Figure 15.

6 Modelling of static response

Static pushover type of analysis was performed for various reinforcement arrangements. Figure 16 shows the comparison of the static numerical pushover curve with the envelope of the cyclic response for the configuration of spiral reinforcement called OY5. This experimental column has the same geometry, boundary conditions and materials used except the spiral pitch is 90 mm instead of 80 mm for all spirals and

has a less ductile rebar for the big spiral ($\varepsilon_u = 0.16$ instead of $\varepsilon_u = 0.22$). This analysis was performed with the same set of material parameters as the OY1 column analysis, and it correctly reproduces the slightly lower confinement effect and ductility than the cyclic model OY1 (see Section 5).

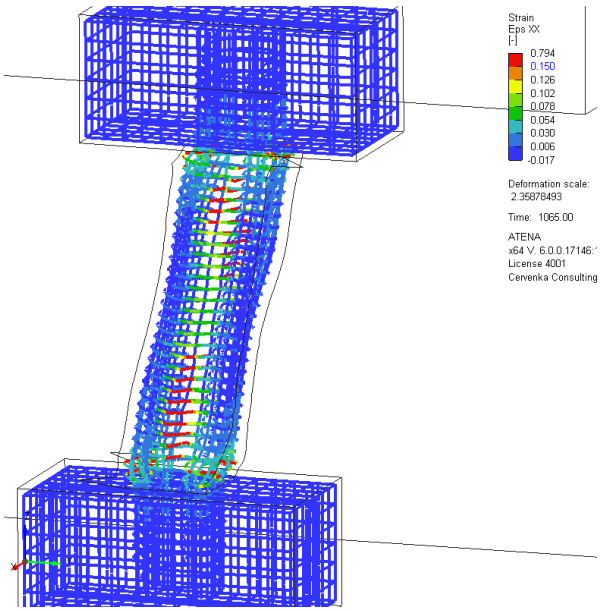

Figure 14: Areas with fractured reinforcement at horizontal displacement of about 165 mm (corresponding drift 6.875 %). Big spiral reinforcement fracture causes failure shortly after.

7 Conclusions

The paper presents a development of a suitable numerical model for the simulation of novel multi-spiral reinforcement for prefabricated reinforced concrete columns. The numerical simulation was performed in the software ATENA [4]. The model is able to capture the important aspects of the behaviour of the columns with multi-spiral reinforcement in static as well as cyclic loading as described in Section 4. The model takes into account the concrete crushing by the plasticity based model with non-associated hardening, the multi-axial stress confinement due to the spiral reinforcement. The fracture-plastic concrete material model [5] uses orthotropic smeared crack formulation to simulate cracked material with crack opening and closing.

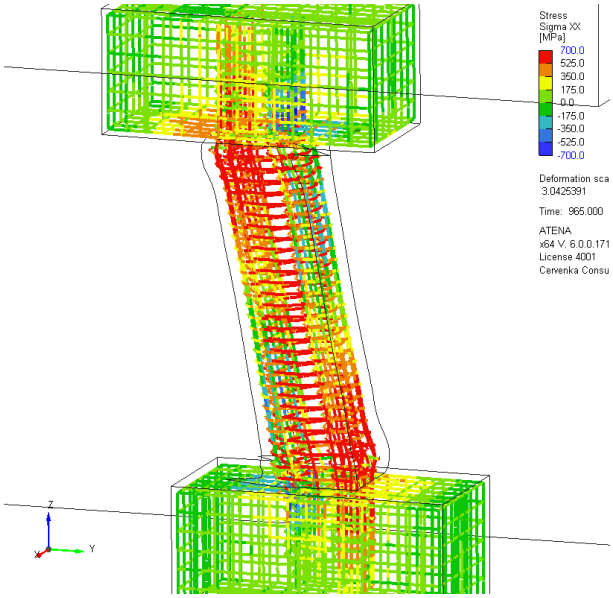

Figure 15: Reinforcement stresses at peak load.

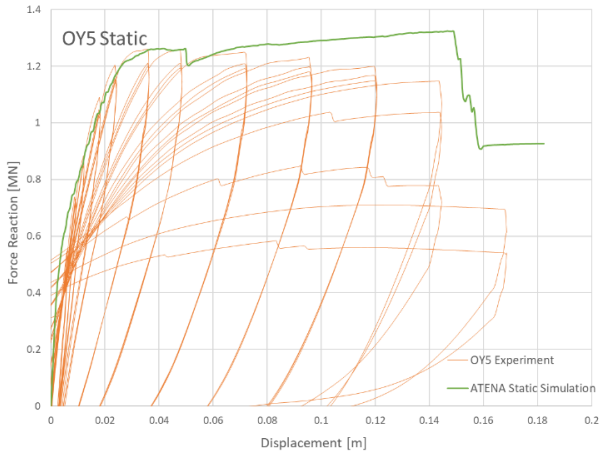

Figure 16: The ATENA Static envelope simulation of the OY5 experiment. the values of peak reaction force correspond, however, the softening trend of the experiment is not achieved. This is probably because the static analysis omits the damage done by cycling loading in crushing and the model therefore hardens instead.

In the cyclic loading, the hysteretic behaviour of the reinforcement is taken into account using Menegotto & Pinto model [15]. The simulations show that cyclic behaviour causes concrete damage by cracking as well as concrete crushing. Even with significant material damage the columns show very low decrease in the load-carrying

capacity due to the confinement effect of the spiral reinforcement. The final failure in the model occurs by rupture of the spiral reinforcement, which is in agreement with the experimental observations. The static envelope simulation shows small hardening rather than gradual softening in the cyclic experiments. This difference can be attributed to the missing damage in the static analysis that is otherwise accumulated during the loading cycles. The numerical results are calculated with basic sets of material parameters that are derived from the known compressive strength of concrete and yield strength of reinforcement. Other material parameters are assumed by their standard values to be able to demonstrate the true predictive nature of the numerical simulation without any fine tunning and fitting of the various model parameters.

The objective of this work is to develop a suitable numerical model for the prediction of the structural behaviour of spiral-reinforced concrete columns that can be applied in the design and the optimization of the prefabricated columns with spiral reinforcement in practice.

Acknowledgement: the work was financially supported by TA ČR project CeSTaR-2 no. TM01000059 - Reducing material demands and enhancing structural capacity of multi-spiral reinforced concrete columns – advanced simulation and experimental validation.

8 References

[1] Kuo, M.T. (2008). *Axial Compression Tests and Optimization Study of 5-Spiral Rectangular RC Columns*. Master Thesis, National Chiao Tung University.

[2] Hsu, W.C. (2019). *Cyclic Behavior of Concrete Columns with Unstressed Steel Strands as Longitudinal Reinforcement*. Master Thesis, National Taiwan University.

[3] Papanikolaou VK, Kappos AJ. Confinement-sensitive plasticity constitutive model for concrete in triaxial compression. International Journal of Solids and Structures. 2007 Oct 15;44(21):7021-48.

[4] Cervenka, V., Jendele, L., Cervenka, J. (2018-2020). *Atena Program Documentation,* Prague, Cervenka Consulting, 2020.

[5] Cervenka J, Papanikolaou VK. Three dimensional combined fracture-plastic material model for concrete. *Int J Plast*. 2008;24:2192–2220. doi.org/10.1016/j.ijplas.2008.01.004.

[6] Menetrey, P. & Willam, K.J. 1995. Triaxial Failure Criterion for Concrete and its Generalization. *ACI Struct. J*. 1995;92:311-8.

[7] Hordijk, D.D. 1991. *Local Approach to Fatigue of Concrete*. Ph.D. Thesis. Delft University of Technology.

[8] Bažant, Z.P. & Oh, B.H., 1983. Crack band theory for fracture of concrete. *Mat. and Structures*, RILEM 16 (3), 155–177.

[9] Cervenka, J., Cervenka, V., Laserna, S., On crack band model in finite element analysis of concrete fracture in engineering practice, *Eng. Fract. Mechanics*, Vol. 197, 2018, pp 27-47, doi.org/10.1016/j.engfracmech.2018. 04.010.

[10] Červenka, V., Margoldová, J., 1995, Tension Stiffening Effect in Smeared Crack Model, *Engineering Mechanics*, S.F. Sture (Eds), 10th Conf., Boulder, Colorado, pp. 655-658.

[11] Slobbe A.T., Hendriks M.A.N., Rots J.G., Systematic assessment of directional mesh bias with periodic boundary conditions: Applied to the crack band model. *Eng. Fract. Mech.*, V. 109, September 2013, pp 186–208.

[12] Bentz, E.C., Vecchio, F.J., Collins, M.P. 2006. Simplified Modified Compression Field Theory for Calculating Shear Strength of Reinforced Concrete Elements. *ACI Material Journal*, Jul/Aug 2006.

[13] Jendele L., Cervenka J., On the Solution of Multi-Point Constraints - Application to FE Analysis of Reinforced Concrete Structures, *Computers and Structures*, doi:10.1016/j.compstruc.2008.04.018. 2007.

[14] Jendele, L., Cervenka, J., Modelling Bar Reinforcement with Finite Bond, *Computers and Structures*, 84, 1780-1791, 2006

[15] Menegotto, M. & Pinto, P.E., 1973. Method of analysis for cyclically loaded RC plane frames including changes in geometry and nonelastic behaviour of elements under combined normal force and bending. Proc. IABSE Symposium, Lisbon, Portugal.